Bull. Chem. Soc. Jpn., 72, 1025—1035 (1999)

Structural Characterization and Magnetic Properties of Triply Carboxylato-Bridged Dinuclear Copper(II) Complexes

Hideaki Matsushima, Masayuki Koikawa, Ryoji Nukada,† Masahiro Mikuriya,† and Tadashi Tokii*

Department of Chemistry and Applied Chemistry, Faculty of Science and Engineering, Saga University, Honjo 1, Saga 840-8502

†Department of Chemistry, School of Science, Kwansei Gakuin University, Uegahara, Nishinomiya 662-8501

(Received November 30, 1998)

A new series of carboxylato-bridged dinuclear copper(II) complexes ($[Cu_2(Ph_2CHCOO)_3(bpy)_2]BF_4$ (**1**), $[Cu_2(Ph_2CHCOO)_3(bpy)_2]CF_3SO_3$ (**2**; blue form), $[Cu_2(Ph_2CHCOO)_3(bpy)_2]CF_3SO_3$ (**3**; green form), $[Cu_2(Ph_2CHCOO)_3(phen)_2]BF_4$ (**4**), $[Cu_2\{(ClPhO)_2CHCOO\}_3(bpy)_2]BF_4$ (**5**), and $[Cu_2\{(ClPhO)_2CHCOO\}_3(bpy)_2]ClO_4$ (**6**), where Ph_2CHCOO, $(ClPhO)_2CHCOO$, bpy, and phen are diphenylacetate anion, bis(4-chlorophenoxy)acetate anion, 2,2′-bipyridine, and 1,10-phenanthroline, respectively) has been prepared. X-Ray crystallographic analyses reveal that complexes **1**—**6** have a triply carboxylato-bridged dicopper(II) core. Two copper(II) ions in **1** and **2** are linked by one familiar "*syn–syn* bridging" carboxylate and two unique "*monatomic* bridging" carboxylates. In **3**—**6**, two "*syn–syn* bridging" carboxylates and one "*monatomic* bridging" carboxylate connect two copper(II) ions. Complexes **2** and **3** are geometrically isometric with each other. Magnetic susceptibility data for the present complexes indicate that a weak antiferromagnetic interaction is operative in each dicopper core in **1**, **2**, **4**, **5**, and **6** with $2J$ values ranging from -5 to -13 cm^{-1}, whereas a ferromagnetic coupling is operative in **3** with a $2J$ value of 9 cm^{-1}.

Over the past few decades, many dicopper(II) complexes have been prepared and the relationships between their magnetic properties and molecular structures have been extensively studied for understanding the spin-exchange interaction. The magneto-structural correlations in di- or polynuclear metal complexes have not yet been completely identified, because the spin-exchange mechanism is affected by several structural parameters, e.g. the metal···metal separation, the bond angles subtended at the bridging atoms, the bridging bond distances, the dihedral angles between the two planes containing metal ions, and the stereochemistries around the metal ions.[1—9] Hatfield and Hodgson have established a linear relationship between the $2J$ value (singlet–triplet energy separation) and the Cu–O–Cu bridging angle in a series of symmetrically di-μ-hydroxo-bridged dinuclear copper(II) complexes.[1] However, the same degree of understanding has not yet been achieved for asymmetrically di-bridged and tri-bridged dinuclear copper(II) complexes. In previous papers,[10] we described both the magnetic properties and the crystal structures of di-μ-carboxylato-bridged dicopper(II) complexes with 1,10-phenanthroline (phen), $[\{Cu(RCOO)(H_2O)(phen)\}_2](NO_3)_2\cdot 4H_2O$ (R = H, CH_3), and found that the strength of the spin-exchange interaction through di-μ-carboxylato-bridges in these compounds was less than only one third of those observed for dinuclear copper(II) carboxylate adducts, $[\{Cu(RCOO)_2L\}_2]$.[2—4] Christou and co-workers[11] have prepared a triply carboxylato-bridged dinuclear copper(II) complex, $[Cu_2(CH_3COO)_3(bpy)_2]ClO_4$ (bpy is 2,2′-bipyridine), with two *syn–syn* bridging acetates (μ-carboxylato-$\varkappa O : \varkappa O'$) and one *monatomic* bridging acetate (μ-carboxylato-$1 : 2\varkappa^2 O$). Interestingly, this compound shows a weak ferromagnetic behavior in a dicopper(II) core. These magnetic features prompted us to investigate the correlation between the structural character and the spin-exchange interaction in such triply carboxylato-bridged dicopper complexes. Moreover, bioinorganic chemists direct their attention to the versatility of the binding modes of carboxylates in metalloprotein active sites.[12] For this purpose, we prepared a new series of triply carboxylato-bridged dicopper(II) complexes, $[Cu_2(RCOO)_3(L)_2]X$, and determined their crystal structures. The complexes described here can be classified into two types based on the crystal structures, as represented schematically by A and B (Chart 1). A preliminary report on the molecular structures and magnetic properties of **1** and **4** has appeared.[13]

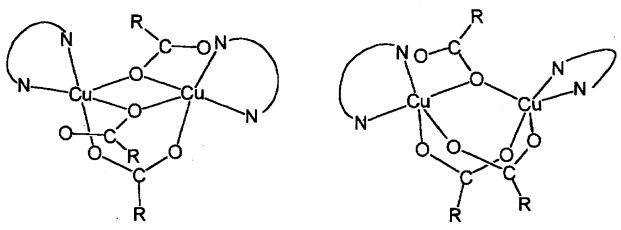

Chart 1.

Experimental

Materials. All ordinary reagents and solvents were purchased and used as received, unless otherwise noted. Methanol was purified by distillation. Acetonitrile was used to measure the absorption spectra after drying over P_2O_5 and distillation.

Caution! Although we have not encountered any problems, it is noted that perchlorate salts are potentially explosive and should be handled in only small quantities with appropriate care.

Preparations. **$[Cu_2(Ph_2CHCOO)_3(bpy)_2]BF_4$ (1).** A 45% aqueous solution of $Cu(BF_4)_2$ (2 mmol) was added to a solution of diphenylacetic acid ($Ph_2CHCOOH$) (2 mmol) and bpy (2 mmol) in 10 cm^3 of an acetonitrile/methanol 1 : 1 mixture under stirring. To the resulting sky-blue solution was added 1 cm^3 of triethylamine under stirring. After the earlier precipitates were filtered off, the filtrate was allowed to stand for one day at room temperature. Deep-blue crystals were collected, washed with acetonitrile, and dried in vacuo. Yield 0.36 g (37%). Anal. Found: C, 64.13; H, 4.36; N, 4.73; Cu, 11.09%. Calcd for $C_{62}H_{49}BCu_2F_4N_4O_6$ (**1**): C, 64.20; H, 4.26; N, 4.83; Cu, 10.96%.

$[Cu_2(Ph_2CHCOO)_3(bpy)_2]CF_3SO_3$ (2; Blue Form) and $[Cu_2(Ph_2CHCOO)_3(bpy)_2]CF_3SO_3$ (3; Green Form). $Ph_2CHCOOH$ (6 mmol) and $Cu(CF_3SO_3)_2$ (4 mmol) were dissolved in 30 cm^3 of methanol, and 6 mmol of triethylamine was added to this solution. To the resulting green solution was added a solution of bpy (4 mmol) in 10 cm^3 of methanol with stirring; immediately, a blue precipitate appeared. The blue precipitate was collected, washed with methanol, dried in air, and recrystallized from methanol/acetonitrile (1 : 1). Deep-blue crystals of **2**·CH_3CN were collected and dried in vacuo. Yield 0.98 g (40%). After the collection of **2**, the filtrate was allowed to stand for 10 d at room temperature. Green crystals of **3** were precipitated. Yield 0.37 g (15%). Anal. Found: C, 61.80; H, 4.03; N, 4.50; Cu, 10.35%. Calcd for $C_{63}H_{49}Cu_2F_3N_4O_9S$ (**2**): C, 61.91; H, 4.04; N, 4.58; Cu, 10.40%. Found: C, 61.91; H, 4.03; N, 4.60; Cu, 10.33%. Calcd for $C_{63}H_{49}Cu_2F_3N_4O_9S$ (**3**): C, 61.91; H, 4.04; N, 4.58; Cu, 10.40%.

$[Cu_2(Ph_2CHCOO)_3(phen)_2]BF_4$ (4). To a solution of $Ph_2CHCOOH$ (1 mmol) and phen·H_2O (1 mmol) in 10 cm^3 of methanol was added a 45% aqueous solution of $Cu(BF_4)_2$ (1 mmol) under stirring; the resulting solution was then adjusted to pH 2.6 with triethylamine. The bluish-green solution was filtered and the filtrate was stored for three days at room temperature. Bluish-green crystals were collected, washed with cold methanol, and dried in air. Yield 0.17 g (43%). Anal. Found: C, 65.57; H, 4.13; N, 4.61; Cu, 10.70%. Calcd for $C_{66}H_{49}BCu_2F_4N_4O_6$ (**4**): C, 65.62; H, 4.09; N, 4.64; Cu, 10.52%.

$[Cu_2\{(ClPhO)_2CHCOO\}_3(bpy)_2]BF_4$ (5). To a solution of bis(4-chlorophenoxy)acetic acid $\{(ClPhO)_2CHCOOH\}$ (2 mmol) and bpy (2 mmol) in 12 cm^3 of methanol/acetonitrile (3 : 1) was added a 45% aqueous solution of $Cu(BF_4)_2$ (2 mmol) under stirring; triethylamine (3 mmol) was then added to the reaction mixture dropwise. The resulting bluish-green solution was filtered and the filtrate was stored for one day at room temperature. Green crystals were collected, washed with cold methanol, and dried in air. Yield 0.40 g (41%). Anal. Found: C, 50.97; H, 2.99; N, 3.85; Cu, 8.49%. Calcd for $C_{62}H_{43}BCl_6Cu_2F_4N_4O_{12}$ (**5**): C, 50.91; H, 2.96; N, 3.83; Cu, 8.69%.

$[Cu_2\{(ClPhO)_2CHCOO\}_3(bpy)_2]ClO_4$ (6). To a solution of $(ClPhO)_2CHCOOH$ (1.5 mmol) and bpy (1 mmol) in 5 cm^3 of acetonitrile was added a solution of $Cu(ClO_4)_2·6H_2O$ (1 mmol) in 5 cm^3 of acetonitrile under stirring; triethylamine (1.5 mmol) was then added to the reaction mixture dropwise. The resulting bluish-green solution was filtered and the filtrate was stored for one day at room temperature. Green crystals were collected, washed with cold methanol, and dried in air. Yield 0.49 g (33%). Anal. Found: C, 50.36; H, 2.98; N, 3.78; Cu, 8.57%. Calcd for $C_{62}H_{43}Cl_7Cu_2N_4O_{16}$ (**6**): C, 50.48; H, 2.94; N, 3.80; Cu, 8.62%.

Physical Measurements. Carbon, hydrogen, and nitrogen analyses were carried out at the Service Center of Elemental Analysis, Kyushu University. The amounts of copper were determined by a titrimetric method. Infrared (IR) spectra were measured with a Perkin Elmer Spectrum 2000 FT-IR spectrophotometer in the region of 4000—600 cm^{-1} on Nujol mulls. Solid-state (diffuse reflectance, 1500—200 nm) and solution electronic spectra (in CH_3CN, 900—400 nm) were recorded on a Perkin Elmer Lamda 19 UV/VIS/NIR spectrophotometer. Magnetic susceptibilities in the 80—300 K temperature range were measured by the Faraday method using a CHAN-1000 microbalance, and those for **2** and **3** in the 3—300 K temperature range were measured on a Quantum Design MPMS-5S SQUID susceptometer. The susceptibilities were corrected for the diamagnetism of the constituent atoms using Pascal's constants.[14] The effective magnetic moments were calculated from the equation, $\mu_{eff} = 2.83\sqrt{(\chi_A - N\alpha)T}$ where χ_A is the atomic magnetic susceptibility and $N\alpha$ is the temperature-independent paramagnetism. The field dependence of the magnetization was measured on polycrystalline samples of **3** up to 4.8 T at 4.5 K.

X-Ray Crystal Structure Determinations. Suitable crystals for **1**·CH_3CN, **3**, **4**, **5**, and **6** were grown from each reaction mixture, as mentioned in the section concerning preparations. Single crystals of **2**·CH_3CN suitable for an X-ray structural analysis were obtained by recrystallization from methanol/acetonitrile (1 : 1). The diffraction data were measured on a Rigaku AFC5S automated four-circle diffractometer with graphite-monochromated Mo $K\alpha$ (λ = 0.71069 Å) radiation. The unit-cell parameters of each crystal were obtained from a least-squares refinement based on 25 high-angle reflections. The data were collected at a temperature of 23±1 °C using the ω scan (**1**·CH_3CN, **2**·CH_3CN) and the ω–2θ scan (**3**—**6**) techniques to a maximum 2θ value of 55° for Mo $K\alpha$ except for **1**·CH_3CN (50°). The weak reflections ($I < 10\sigma(I)$) were rescanned (maximum 2 rescans) and the counts were accumulated to assure good counting statistics. Stationary background counts were recorded on each side of the reflection. The ratio of the peak counting time was 2 : 1. The intensities of three representative reflections, which were measured after every 150 reflections, remained constant throughout the data collection, indicating both crystal and electronic stability (no decay correction was applied).

An empirical absorption correction, based on azimuthal scans of several reflections, was applied, which resulted in transmission factors ranging from 0.92 to 1.00 for **1**·CH_3CN, from 0.83 to 1.00 for **2**·CH_3CN, from 0.93 to 1.00 for **3**, from 0.92 to 1.00 for **4**, from 0.94 to 1.00 for **5**, and from 0.91 to 1.00 for **6**. The data were corrected for both Lorentz and polarization effects. The crystallographic data and collection details are summarized in Table 1.

The structure was solved by direct methods[15] (MITHRIL or SIR, and DIRDIF). The non-hydrogen atoms were refined anisotropically, except for the following eight atoms of **1**·CH_3CN: two carbon atoms (C63, C64) and one nitrogen atom (N5) of a crystal solvent molecule of acetonitrile and all fluorine atoms {F1, F2, F3, F4(A and B)} and one boron atom (B1) of a tetrafluoroborate anion. One of the fluorine atoms of BF_4^- in **1**·CH_3CN shows a disorder; thus, site-occupancy factors for F4A and F4B were determined on the basis of the peak intensities in a difference Fourier map to 0.7 and 0.3, respectively. All hydrogen atoms were located on the calculated positions. Refinements were carried out by a full-matrix least-

Table 1. Crystallographic Data and Collection Details

	1·CH_3CN	**2**·CH_3CN	**3**	**4**	**5**	**6**
Formula	$C_{64}H_{52}BCu_2F_4N_5O_6$	$C_{65}H_{52}Cu_2F_3N_5O_9S$	$C_{63}H_{49}Cu_2F_3N_4O_9S$	$C_{66}H_{49}BCu_2F_4N_4O_6$	$C_{62}H_{43}BCl_6Cu_2F_4N_4O_{12}$	$C_{62}H_{43}Cl_7Cu_2N_4O_{16}$
F. W.	1201.04	1263.30	1222.25	1208.03	1462.66	1475.30
Crystal dimensions/mm	0.80 × 0.60 × 0.90	0.70 × 0.70 × 0.70	0.30 × 0.20 × 0.40	0.50 × 0.35 × 0.60	0.20 × 0.15 × 0.30	0.25 × 0.15 × 0.40
Crystal system	Monoclinic	Monoclinic	Triclinic	Triclinic	Triclinic	Triclinic
Space group	$P2_1/c$	$P2_1/c$	$P\bar{1}$	$P\bar{1}$	$P\bar{1}$	$P\bar{1}$
a/Å	14.803(5)	15.169(4)	13.571(7)	13.683(8)	16.034(6)	16.00(1)
b/Å	13.151(6)	13.087(5)	17.905(8)	18.163(2)	18.270(7)	18.276(9)
c/Å	29.898(7)	30.25(1)	13.372(8)	13.204(3)	12.584(3)	12.624(2)
α/°			102.15(4)	105.86(1)	106.97(2)	106.90(2)
β/°	98.96(3)	97.30(3)	109.59(4)	110.28(3)	92.18(3)	92.01(5)
γ/°			106.36(4)	100.18(3)	114.82(3)	114.78(6)
V/Å^3	5750(3)	5957(4)	2765(3)	2823(2)	3145(2)	3154(3)
Z	4	4	2	2	2	2
D_c/g cm^{-3}	1.387	1.408	1.468	1.421	1.544	1.553
$F(000)$	2472	2600	1256	1240	1480	1496
μ(Mo $K\alpha$)/cm^{-1}	8.08	8.17	8.77	8.22	10.08	10.44
No. of independent reflections	10631 (R_{int} = 0.031)	8864 (R_{int} = 0.052)	12676 (R_{int} = 0.049)	12958 (R_{int} = 0.050)	8568 (R_{int} = 0.084)	10409 (R_{int} = 0.078)
No. of observations ($I > 3\sigma(I)$)	5006	4172	4994	5937	3744	4015
No. of variables	703	762	739	748	820	820
Final residuals[a)]						
R, R_w	0.058, 0.068	0.048, 0.051	0.056, 0.061	0.049, 0.055	0.054, 0.058	0.054, 0.058
Largest peak in final Diff. fourier/e Å^{-3}	0.70	0.41	0.57	0.62	0.43	0.51

a) $R = \Sigma||F_o| - |F_c||/\Sigma|F_o|$ and $R_w = [\Sigma w(|F_o| - |F_c|)^2/\Sigma wF_o^2]^{1/2}$.

squares method.[16] The final discrepancy factors (R and R_w) are listed in Table 1.

The neutral-atom scattering factors were taken from Cromer and Waber.[17] Anomalous dispersion effects were included in F_c;[18] the values for $\Delta f'$ and $\Delta f''$ were those of Cromer.[19] All calculations were performed using the TEXSAN[20] crystallographic software package of Molecular Structure Corporation. The final positional and thermal parameters, full listings of bond distances and angles, and the $F_o - F_c$ tables have been deposited as Document No. 72014 at the Office of the Editor of Bull. Chem. Soc. Jpn.

Results and Discussion

Description of Crystal Structures. Type A: $[Cu_2(Ph_2CHCOO)_3(bpy)_2]BF_4 \cdot CH_3CN$ (1·CH_3CN) and $[Cu_2(Ph_2CHCOO)_3(bpy)_2]CF_3SO_3 \cdot CH_3CN$ (2·CH_3CN; Blue Form). Both complexes 1·CH_3CN and 2·CH_3CN have a solvated acetonitrile molecule crystallized in the monoclinic space group $P2_1/c$. The structure of the complex cation of 2·CH_3CN is shown in Fig. 1, and selected bond distances and angles for 1·CH_3CN and 2·CH_3CN are listed in Table 2.

The complexes consist of a dicopper(II) core with three diphenylacetate bridges and two bidentate ligands of bpy, and a counter mono-anion. As for 2·CH_3CN, a $CF_3SO_3^-$ ion instead of a BF_4^- ion in 1·CH_3CN is included in the crystallographically asymmetric unit. The coordination around each copper(II) ion is essentially a square pyramidal (SP) geometry with the basal plane comprising two nitrogen atoms from bpy and two oxygen atoms from carboxylates; also,

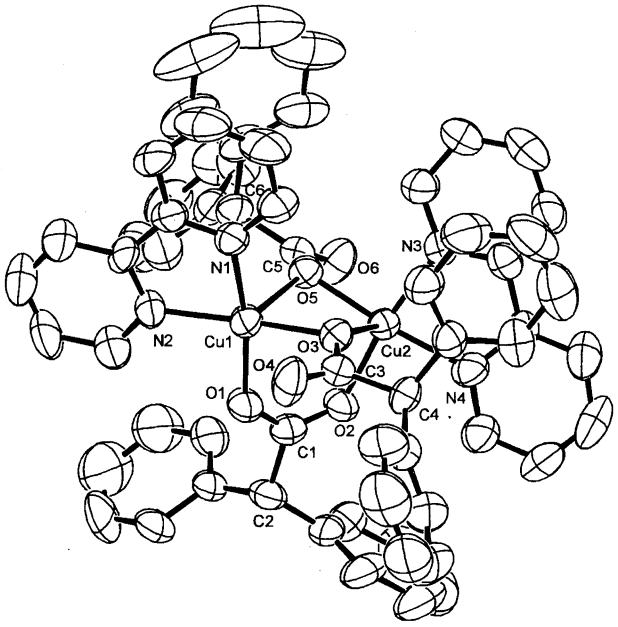

Fig. 1. An ORTEP drawing for the complex cation of 2·CH_3CN. Hydrogen atoms are not shown for clarity.

each axial site is occupied by a monatomically bridged carboxylate oxygen atom (O5 for Cu1 and O3 for Cu2). This assignment concerning the coordination geometry is supported by the structural index τ, $\tau = (\alpha - \beta)/60°$, where α and β are the two largest angles ($\alpha > \beta$) around a five-coordinated metal center, proposed by Addison et al.[21] For a

Table 2. Selected Bond Distances (Å) and Angles (°) for 1·CH_3CN and 2·CH_3CN

	1·CH_3CN	2·CH_3CN		1·CH_3CN	2·CH_3CN
Distances/Å					
Cu1–O1	1.937(5)	1.936(4)	Cu2–O2	1.959(5)	1.957(4)
Cu1–O3	1.959(4)	1.962(4)	Cu2–O3	2.269(5)	2.270(5)
Cu1–O5	2.316(5)	2.313(5)	Cu2–O5	1.957(4)	1.949(4)
Cu1–N1	1.968(6)	1.973(6)	Cu2–N3	1.984(6)	1.987(6)
Cu1–N2	1.996(6)	1.992(6)	Cu2–N4	1.987(6)	1.978(6)
Cu1···O4	2.846(5)	2.809(6)	Cu2···O6	2.908(5)	2.891(5)
C1–O1	1.267(8)	1.273(8)	C5–O5	1.303(8)	1.274(8)
C1–O2	1.230(8)	1.227(8)	C5–O6	1.223(8)	1.220(8)
C3–O3	1.286(8)	1.279(8)	Cu1···Cu2	3.146(2)	3.149(2)
C3–O4	1.212(8)	1.218(8)			
Angles/°					
O1–Cu1–O3	91.7(2)	91.8(2)	O5–Cu2–O2	92.2(2)	92.2(2)
O1–Cu1–N1	168.3(2)	170.8(2)	O5–Cu2–N3	94.7(2)	95.1(2)
O1–Cu1–N2	89.5(3)	90.9(2)	O5–Cu2–N4	170.4(2)	171.9(2)
O1–Cu1–O5	93.5(2)	92.3(2)	O5–Cu2–O3	80.2(2)	80.3(2)
O3–Cu1–N1	97.1(3)	95.7(2)	O2–Cu2–N3	171.2(2)	170.8(2)
O3–Cu1–N2	174.4(2)	171.1(2)	O2–Cu2–N4	91.3(2)	91.2(2)
O3–Cu1–O5	78.9(2)	78.9(2)	O2–Cu2–O3	90.4(2)	90.0(2)
N1–Cu1–N2	80.9(3)	80.9(3)	N3–Cu2–N4	81.1(3)	80.8(3)
N1–Cu1–O5	95.7(2)	94.5(2)	N3–Cu2–O3	96.1(2)	96.8(2)
N2–Cu1–O5	106.4(2)	109.4(2)	N4–Cu2–O3	108.8(2)	107.0(2)
Cu1–O1–C1	128.0(5)	128.7(5)	Cu2–O2–C1	131.0(5)	131.0(5)
Cu1–O3–C3	114.0(4)	112.6(4)	Cu2–O3–C3	139.1(5)	141.8(5)
Cu1–O5–C5	140.3(4)	138.9(4)	Cu2–O5–C5	115.8(4)	115.4(4)
Cu1–O3–Cu2	95.9(2)	95.9(2)	Cu1–O5–Cu2	94.4(2)	94.9(2)

perfectly SP geometry τ is equal to 0, while it becomes 1 for a perfectly trigonal bipyramidal (TBP) geometry. The application of this approach to each copper(II) ion of **1**·CH_3CN and **2**·CH_3CN yields the value sets of (τ_{Cu1}, 0.01; τ_{Cu2}, 0.10) and (τ_{Cu1}, 0.01; τ_{Cu2}, 0.02), respectively. The deviation of copper(II) ions from the corresponding least-squared N_2O_2 planes toward the apical direction falls in the range of 0.11—0.12 Å and the Cu–O distances at the axial sites are considerably longer by 0.31—0.38 Å than those in the basal plane, as expected.

One of the bridging carboxylates has the well-known bidentate *syn–syn* bridging mode, and the others have the unique *monatomic* bridging mode, forming a novel carboxylato-linkage. This carboxylato-linkage is known only in $[Cu_2(CH_3COO)_3(BIPhMe)_2]BF_4 \cdot 3H_2O$ {BIPhMe = bis(1-methylimidazole-2-yl)phenylmethoxymethane}.[22] The bridging angles (Cu1–O3–Cu2 and Cu1–O5–Cu2) of the monatomically bridged oxygen atoms are 95.9(2)° and 94.4(2)° for **1**·CH_3CN and 95.9(2)° and 94.9(2)° for **2**·CH_3CN, respectively. Although these angles are comparable to those observed in the complexes, [{Cu(5-R-L)(CH_3COO)}$_2$] (5-R-L$^-$ = anions of *N*-methyl-*N*′-{salicyliden or 5-substituted (methoxy, nitro, or bromo)-salicyliden}-1,3-propanediamine),[23—25] which have a doubly *monatomic* bridging structure, the Cu···Cu separations of **1**·CH_3CN (3.146(2) Å) and **2**·CH_3CN (3.149(2) Å) are notably shorter than those in [{Cu(5-R-L)(CH_3COO)}$_2$] (3.38—3.51 Å). This shortening of the Cu···Cu separations is attributed to the presence of the additional carboxylato-bridging; two copper(II) ions are brought closer to each other by the binding of the third carboxylate with the *syn–syn* mode. Furthermore this additional bridging also causes some deviation from co-planarity of the four-membered Cu_2O_2 (Cu1, Cu2, O3, O5) bridging units in **1**·CH_3CN and **2**·CH_3CN. Bending is found at the O3···O5 axis on the Cu_2O_2 unit, and the dihedral angles between the [Cu1, O3, O5] and [Cu2, O3, O5] planes are 147.4° and 148.5° in **1**·CH_3CN and **2**·CH_3CN, respectively.

In the *monatomic* bridging carboxylates of **1**·CH_3CN and **2**·CH_3CN, the C3–O3 and C5–O5 distances appear to be somewhat longer than the C3–O4 and C5–O6 distances, indicating the presence of some double-bond character in the C3–O4 and C5–O6 bonds. The Cu1···O4 and Cu2···O6 separations in **1**·CH_3CN and **2**·CH_3CN range over 2.81—2.91 Å, and are fairly longer than those of [{Cu(5-R-L)(CH_3COO)}$_2$] (2.50—2.67 Å).[23—25] These results suggest that the sixth coordination from the oxygen atoms (O4 and O6) of *monatomic* bridging carboxylates toward each copper(II) ion is very weak.

Type B: $[Cu_2(Ph_2CHCOO)_3(bpy)_2]CF_3SO_3$ (3; Green Form), $[Cu_2(Ph_2CHCOO)_3(phen)_2]BF_4$ (4), $[Cu_2\{(ClPhO)_2CHCOO\}_3(bpy)_2]BF_4$ (5), and $[Cu_2\{(ClPhO)_2CHCOO\}_3(bpy)_2]ClO_4$ (6). All of complexes **3**, **4**, **5**, and **6** crystallized in the triclinic space group $P\bar{1}$. In particular, the unit-cell parameters of **5** and **6** are very similar, as presented in Table 1. The structures of the complex cations of **3**, **4**, and **6** are shown in Figs. 2, 3, and 4, respectively. Selected bond distances and angles for **3**, **4**, **5**, and **6** are summarized in Table 3.

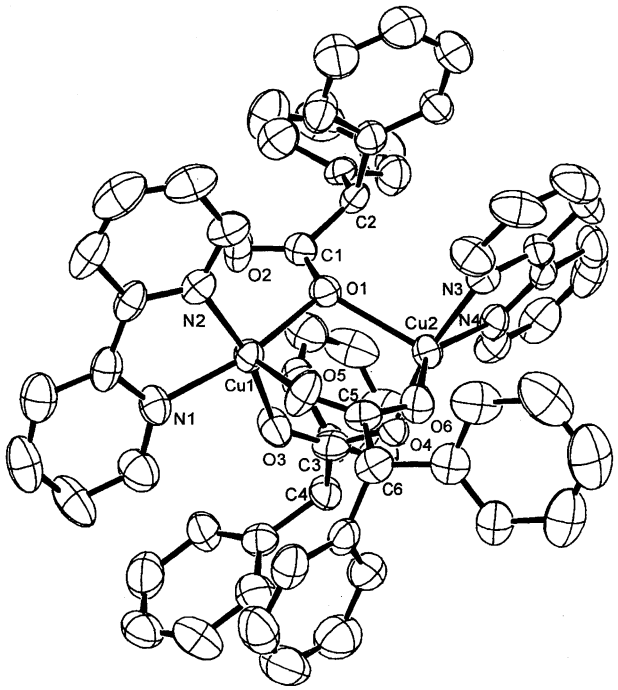

Fig. 2. An ORTEP drawing for the complex cation of **3**.

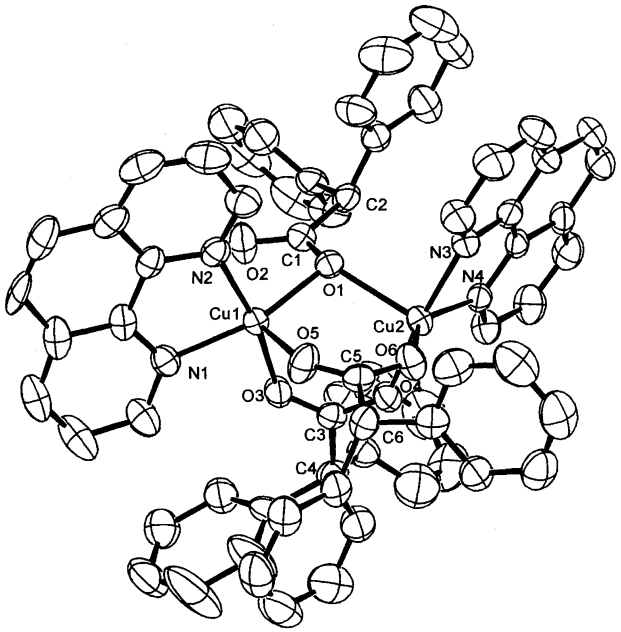

Fig. 3. An ORTEP drawing for the complex cation of **4**.

Each triply bridged dinuclear core contains two copper(II) ions linked by three carboxylato ligands. These carboxylato ligands have formed two bidentate *syn–syn* bridging modes and one *monatomic* bridging mode. Terminal bidentate ligands (bpy for **3**, **5**, **6** and phen for **4**) complete a five-coordination at each copper(II) center. Complexes **2** and **3** are geometrically isometric with each other.

A few examples having such a structural feature have been found in several transition-metal complexes.[12,26] In copper-

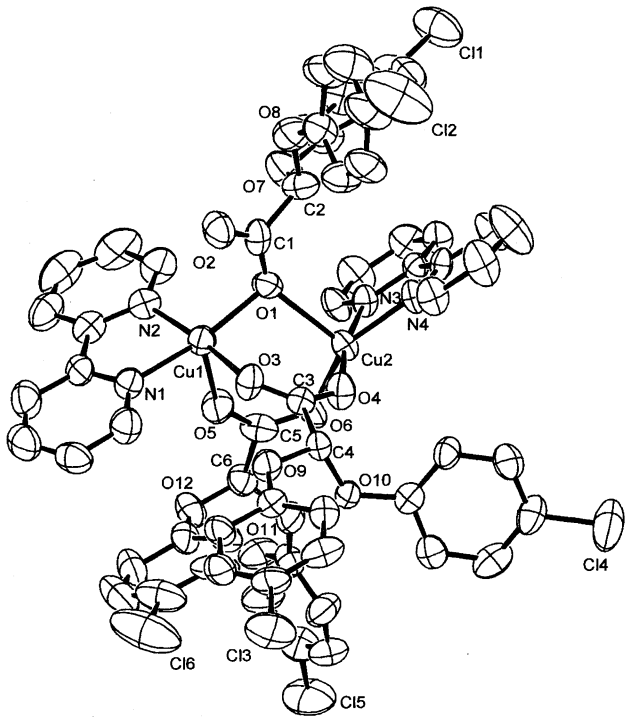

Fig. 4. An ORTEP drawing for the complex cation of **6**.

(II) chemistry, the triply benzoato-bridged one-dimensional copper(II) polymer, $\{[Cu_2(PhCOO)_3(bppz)]ClO_4\cdot(H_2O)_2\}_n$, where bppz = 2,5-bis(2-pyridyl)pyrazine, in which the dicopper core is linked by bppz ligand, has been reported[27] quite recently. To the best of our knowledge, as one example of the triply carboxylato-bridged dinuclear copper(II) complexes, the $[Cu_2(CH_3COO)_3(bpy)_2]ClO_4$ complex has been reported.[11]

As can be seen from the τ_{Cu1} values of 0.06 for **3**, 0.17 for **4**, 0.07 for **5**, and 0.06 for **6**, the environment of Cu1 in each complex is assigned to a SP geometry with O5 at the apical position. These copper(II) ions lie 0.10—0.25 Å apart from the N1, N2, O1, O3 least-squares planes toward the apical direction. Judging from the values of τ_{Cu2} (0.35 for **3**, 0.39 for **4**, 0.29 for **5**, 0.28 for **6**), the geometry around Cu2 is better described as an extremely distorted square pyramid with O4, O6, N3, and N4 in the basal plane and O1 at the apex. Therefore, the bridging oxygen atom (O1) of monatomically bridged carboxylate simultaneously occupied a basal coordination site of one copper(II) ion and an apical coordination site of another copper(II) ion. The oxygen atoms O5 and O6 of one bidentate *syn–syn* carboxylate also linked between an apical site of Cu1 and a basal site of Cu2. The distances from each copper(II) ion to the apical oxygen atom are longer than the in-plane Cu–O distances. The deviation (0.36 Å for **3**, 0.32 Å for **4**, 0.32 Å for **5**, 0.32 Å for **6**) of Cu2 from each basal plane is larger than those of Cu1 and reflects greater distortion of the coordination geometry.

The Cu···Cu distances in **3** (3.408(2) Å), **5** (3.408(2) Å), and **6** (3.413(3) Å) are almost comparable to that in the acetato-bridged complex (3.392(2) Å),[11] but somewhat longer than that in **4** (3.357(2) Å). It is noteworthy that the

Table 3. Selected Bond Distances (Å) and Angles (°) for **3**, **4**, **5**, and **6**

	3	**4**	**5**	**6**
Distances/Å				
Cu1–O1	1.986(5)	2.030(4)	1.967(7)	1.969(7)
Cu1···O2	2.775(6)	2.550(4)	2.701(8)	2.715(8)
Cu1–O3	1.952(5)	1.961(4)	1.946(7)	1.955(7)
Cu1–O5	2.132(5)	2.136(4)	2.173(8)	2.169(7)
Cu1–N1	2.012(6)	2.017(4)	1.989(8)	1.975(8)
Cu1–N2	1.999(6)	2.009(5)	1.983(9)	1.980(8)
Cu2–O1	2.259(5)	2.232(4)	2.318(8)	2.314(8)
Cu2–O4	1.923(5)	1.939(4)	1.947(7)	1.950(6)
Cu2–O6	1.943(5)	1.936(4)	1.947(7)	1.942(7)
Cu2–N3	1.984(6)	2.005(5)	1.992(7)	1.984(8)
Cu2–N4	2.045(6)	2.043(4)	1.998(8)	2.008(7)
C1–O1	1.294(8)	1.294(6)	1.27(1)	1.27(1)
C1–O2	1.217(8)	1.218(6)	1.20(1)	1.22(1)
C3–O3	1.254(8)	1.241(6)	1.23(1)	1.24(1)
C3–O4	1.252(8)	1.262(6)	1.25(1)	1.24(1)
C5–O5	1.226(8)	1.232(6)	1.20(1)	1.22(1)
C5–O6	1.269(8)	1.262(6)	1.24(1)	1.23(1)
Cu1···Cu2	3.408(2)	3.357(2)	3.408(2)	3.413(3)
Angles/°				
O1–Cu1–N1	162.9(2)	158.9(2)	168.9(3)	169.7(3)
O1–Cu1–O5	96.3(2)	100.3(2)	99.0(3)	98.3(3)
O3–Cu1–N2	166.2(2)	168.9(2)	172.9(4)	173.0(3)
O3–Cu1–O5	101.5(2)	96.6(2)	95.8(3)	94.9(3)
O5–Cu1–N1	100.5(2)	100.7(2)	91.2(3)	91.1(3)
O5–Cu1–N2	88.0(2)	90.3(2)	85.5(3)	86.3(3)
N1–Cu1–N2	79.9(3)	81.7(2)	81.3(4)	81.7(4)
O1–Cu2–N3	97.1(2)	93.3(2)	99.3(3)	98.8(3)
O1–Cu2–N4	109.0(2)	102.0(2)	99.6(3)	98.9(3)
O1–Cu2–O4	92.7(2)	91.8(1)	89.8(3)	90.1(3)
O1–Cu2–O6	103.7(2)	110.0(2)	109.0(3)	108.6(3)
O4–Cu2–N3	167.6(2)	171.1(2)	168.7(3)	169.1(3)
O6–Cu2–N4	146.7(2)	147.7(2)	151.1(3)	152.1(3)
N3–Cu2–N4	79.9(2)	81.5(2)	80.6(3)	80.9(3)
Cu1–O1–Cu2	106.7(2)	103.8(2)	105.1(3)	105.4(3)
Cu1–O1–C1	109.6(4)	101.7(3)	107.6(7)	106.8(7)
Cu2–O1–C1	132.5(4)	139.1(3)	140.6(7)	141.1(7)
Cu1–O3–C3	135.2(5)	130.9(4)	132.4(7)	131.7(6)
Cu2–O4–C3	131.3(5)	134.2(4)	133.8(7)	134.2(7)
Cu1–O5–C5	133.7(5)	138.6(4)	137.5(8)	139.3(7)
Cu2–O6–C5	130.5(5)	126.9(4)	124.7(8)	125.9(7)

Cu···Cu distances in dinuclear copper(II) complexes with only carboxylate bridges relates with the number and the mode of the bridging carboxylate: $[\{Cu(RCOO)_2L\}_2]$,[2–4] four *syn–syn* carboxylates (ca. 2.6 Å)≪$[\{Cu(RCOO)(phen$ or $bpy)\}_2]^{2+}$,[10,28] two *syn–syn* carboxylates (ca. 3.05 Å) < **1** and **2**, two *monatomic* and one *syn–syn* carboxylates (ca. 3.15 Å) < **3**, **4**, **5**, **6**, and $[Cu_2(CH_3COO)_3(bpy)_2]ClO_4$,[11] one *monatomic* and two *syn–syn* carboxylates (ca. 3.38 Å) < $[\{Cu(5\text{-R-L})(CH_3COO)\}_2]$,[23–25] two *monatomic* carboxylates (ca. 3.47 Å). There are considerable differences between the Cu1–O1 and Cu2–O1 distances in **3**—**6**. In **4**, the Cu1–O1 distance is 2.030(4) Å and the Cu2–O1 distance is 2.232(4) Å. The former is longest and the latter is shortest in the corresponding distances in this series of complexes. This charac-

teristic feature of the Cu–O1 distances in **4** may be attributed to the intra-molecular π–π stacking interaction.[10,28,29] One phenyl-ring of the *monatomic* bridging carboxylate and the phenanthroline-ring coordinated to Cu2 site in **4** are arranged nearly parallel (5.6°) and eclipsed by each other with the separation of ca. 3.5 Å. The intra-molecular π–π stacking interaction has drawn the *monatomic* bridging carboxylate to Cu2 side shortening the Cu2–O1 bond, and brought about the elongation of the Cu1–O1 bond. Such a stacking interaction has not been observed in other three complexes. This structural feature suggests that the π–π stacking interaction of phen is more efficient than that of bpy.

The Cu1–O1–Cu2 bridging angles in **3**, **4**, **5**, and **6**, ranging from 103.8(2)° to 106.7(2)°, are slightly smaller than the corresponding angle of $[Cu_2(CH_3COO)_3(bpy)_2]ClO_4$ (109.8(1)°).[11] Moreover, the Cu1–O1–C1 and the Cu2–O1–C1 angles in **3**—**6** fall into a wide range of 101.7(3)—109.6(4)° and 132.5(4)—141.1(7)°, respectively. In particular, the difference between the Cu1–O1–C1 (101.7(3)°) and Cu2–O1–C1 (139.1(3)°) angles in **4** is very large compared with those in the other three complexes, and the C1–O1 axis leans toward the Cu1 site. Furthermore the Cu1···O2 separation of 2.550(4) Å in **4** is considerably shorter than those in **3** (2.755(6) Å), **5** (2.701(8) Å), and **6** (2.715(8) Å), indicating an apparent coordination of dangling carboxylate oxygen O2 to the sixth vacant site of Cu1 in **4**. As for the coordination of *syn–syn* bridging carboxylates in **3**—**6**, there are considerable variations in the Cu–O–C angle (124.7(8)—139.3(7)°). Although this contrasts sharply with the situations in $[\{Cu(RCOO)_2L\}_2]$ (the Cu–O–C angles are usually in the range of 122—126°),[2–4,7] similar variations have been confirmed in $[Cu_2(CH_3COO)_3(bpy)_2]ClO_4$ (129.7(2)—134.2(2)°),[11] $\{[Cu_2(PhCOO)_3(bppz)]ClO_4\cdot(H_2O)_2\}_n$ (124.7(4)—132.2(4)°),[27] and also $[Cu_2(OH)(HCOO)_2(bpy)_2]BF_4$ (123.9(4)—131.4(4)°)[30] which has μ-hydroxo-bis(μ-carboxylato)bridged dicopper(II) core.

These results show the flexibility of coordination of the *monatomic* bridging carboxylate which can bind to metal ions with various bond distances and angles, and suggest that such *monatomic* bridging carboxylates must play an important role in metalloprotein active sites, e.g. the regulation of the metal–metal distance, the control of the metal coordination geometry, and etc.

IR and Electronic Spectroscopy. IR spectral data are listed in Table 4. Since the present complexes possess two different types of carboxylate bridges, two bands were observed for each of the asymmetric and symmetric carboxylate stretching, ν_{as}(COO) and ν_s(COO). The COO stretching bands of **1** and **2** were observed at (ν_{as}(COO): 1635, 1603 cm^{-1}; ν_s(COO): 1402, 1377 cm^{-1}) and (ν_{as}(COO): 1641, 1603 cm^{-1}; ν_s(COO): 1404, 1377 cm^{-1}), respectively. Band assignments for the carboxylate coordination mode can be made on the basis of the separation (Δ_{as-s}) between the ν_{as}(COO) and ν_s(COO) frequencies; the Δ_{as-s} values for the *syn–syn* bridging modes are close to, or slightly less than, those for ionic carboxylates (235 cm^{-1} for ionic diphenylacetates and 200 cm^{-1} for ionic bis(4-chlorophenoxy)acetates), and the Δ_{as-s} values≫ca. 200 cm^{-1} are expected for the *unidentate* binding modes or highly asymmetrical bridging modes.[31] Therefore, the bands at (1603, 1402 cm^{-1}, Δ_{as-s} = 201 cm^{-1} (**1**)) and (1603, 1404 cm^{-1}, Δ_{as-s} = 201 cm^{-1} (**2**)) are assigned to the *syn–syn* bridging carboxylates, and the higher frequency bands of ν_{as}(COO), 1635 cm^{-1} (**1**) and 1641 cm^{-1} (**2**), and the lower frequency band of ν_s(COO), 1377 cm^{-1} (**1** and **2**), are assigned to the *monatomic* bridging carboxylates (Δ_{as-s} = 258 cm^{-1} (**1**), 264 cm^{-1} (**2**)). The ν_s(COO) of **3** and **4** for the *monatomic* and *syn–syn* bridging carboxylates exhibit the same frequency at 1398 and 1378 cm^{-1}, respectively, however, ν_{as}(COO) for each mode is somewhat different; 1640 cm^{-1} (**3**) and 1627 cm^{-1} (**4**) for the *monatomic* mode and 1616 cm^{-1} (**3**) and 1600 cm^{-1} (**4**) for the *syn–syn* mode. Thus, Δ_{as-s} for the *monatomic* and *syn–syn* modes are 262 and 218 cm^{-1} for **3**, and 250 and 202 cm^{-1} for **4**, respectively. In **3** and **4**, the observed difference (12—16 cm^{-1}) in Δ_{as-s} for each mode reflects slight differences in the geometry of the *monatomic* and *syn–syn* bridging carboxylates. The ν_{as}(COO) and ν_s(COO) bands assigned to the *monatomic* and *syn–syn* bridging carboxylate of **5** (*monatomic* mode: 1675 and 1438 cm^{-1} (Δ_{as-s} = 237 cm^{-1}); *syn–syn* mode: 1665 and 1447 cm^{-1} (Δ_{as-s} = 218 cm^{-1})) and **6** (*monatomic* mode: 1675 and 1438 cm^{-1} (Δ_{as-s} = 237 cm^{-1}); *syn–syn* mode: 1662 and 1450 cm^{-1} (Δ_{as-s} = 212 cm^{-1})) were observed in almost identical frequency regions.

Table 4. IR Spectral Data (cm^{-1}) for **1**—**6**

Complex	ν(COO)		Δ(as–s)	BF_4^-	$CF_3SO_3^-$	ClO_4^-
	as	s				
1	1635	1377	258	1060		
	1603	1402	201			
2	1641	1377	264		1278, 1160, 637	
	1603	1404	201			
3	1640	1378	262		1278, 1154, 638	
	1616	1398	218			
4	1627	1378	249	1061		
	1600	1398	202			
5	1675	1438	237	1060		
	1665	1447	218			
6	1675	1438	237			1093, 623
	1662	1450	212			

Complexes **1**, **4**, and **5** show an intense vibration at ca. 1060 cm^{-1} characteristic of a tetrafluoroborate ion. The three bands at ca. 1280, ca. 1160, ca. 640 cm^{-1} in both **2** and **3** are assigned to the vibrations of a trifluoromethansulfonate ion. The typical stretching bands of a perchlorate ion were observed at ca. 1093 and 623 cm^{-1} in **6**.

Electronic spectral data are listed in Table 5. In the solid-state electronic spectra, **1** and **2** exhibit a very similar spectral feature reflecting a structural resemblance to each other. The somewhat broad band and a shoulder were observed at ca. 15.7×10^3 and ca. 10.8×10^3 cm^{-1}, respectively. The separation between these two peaks, $\Delta\tilde{\nu}\approx4.9\times10^3$ cm^{-1}, is typical for a slightly distorted SP geometry.[32] The spectra

Table 5. Electronic Spectral Data (10^3 cm^{-1}) for **1**—**6**

Complex	Solid-state $\tilde{\nu}$	Solid-state $\tilde{\nu}$	Solid-state $\Delta\tilde{\nu}$	Solution-state[a] $\tilde{\nu}$ (ε_M[b])
1	15.63	10.7	4.9	14.50 (131)
2	15.82	11.0	4.8	14.50 (131)
3	14.04			14.50 (133)
4	13.34			14.30 (126)
5	14.88			14.76 (127)
6	14.96			14.75 (127)

a) in CH_3CN. b) $mol^{-1}\,dm^3\,cm^{-1}$.

of **3**—**6**, having the type-B structure, are also similar to one another. Numerous transitions are expect in the d–d range, owing to the coexistence of two copper(II) ions possessing different coordination environments within these complex cations, which cause their band assignments to complicate. As a consequence, one broad maximum was observed in each spectrum at 14.0×10^3, 13.3×10^3, 14.9×10^3, and 15.0×10^3 cm^{-1} for **3**, **4**, **5**, and **6**, respectively. These band maxima are lower in energy compared to those found in **1** and **2**, because the distortion of the metal geometry in **3**—**6** increases from SP to TBP. It is reasonable that the red sift of this band becomes greater with increasing τ values of **3**—**6**.

The spectral features of **1**—**6** in acetonitrile are quite similar to one another, and slightly different from those in solid-state. The d–d bands of the two sets of complexes, (**1**, **2**, **3**) and (**5**, **6**), in which the carboxylates are same, were observed at 14.5×10^3 and 14.8×10^3 cm^{-1}, respectively. The difference between the solid-state and solution spectra of **1**—**6** suggest that some structural changes may occur in a solution, and that the remarkable structural differences of **1**—**6** in crystals do not preserve in a solution.[11,33]

Magnetic Properties. Magnetic susceptibility measurements were carried out in the temperature range of 80—300 K for **1**, **4**, **5**, and **6**, and 3—300 K for **2** and **3**. The temperature dependence of the magnetic susceptibilities (χ_A) and the effective magnetic moments (μ_{eff}) per Cu(II) ion of **2** and **3** are representatively shown in Figs. 5 and 6, respectively. The susceptibility data for **2** exhibit a maximum at 8.0 K. The μ_{eff} values for **1** and **2** having the type-A structure gradually decrease with decreasing temperature from 1.91 B.M. (294.8 K) and 1.88 B.M. (299.9 K) to 1.87 B.M. (81.2 K) and 0.43 B.M. (3.0 K), respectively. The same magnetic behavior was also observed for **4**, **5**, and **6** with the type-B structure. In contrast, the magnetic susceptibility data for **3** show typical ferromagnetic behavior; the μ_{eff} values gradually increase with decreasing temperature from 1.88 B.M. at 299.9 K to 1.95 B.M. at 85.0 K, and reach 2.19 B.M at 3.0 K. The magnetic data for the present complexes are well represented by the Bleaney–Bowers equation,[34]

$$\chi_A = \frac{Ng^2\beta^2}{kT}\left[3+\exp\left(\frac{-2J}{kT}\right)\right]^{-1} + N\alpha, \qquad (1)$$

where χ_A is the susceptibility per copper(II) ion, $-2J$ is equal to the energy separation between the spin-singlet and the spin-triplet states based on the isotropic spin-exchange

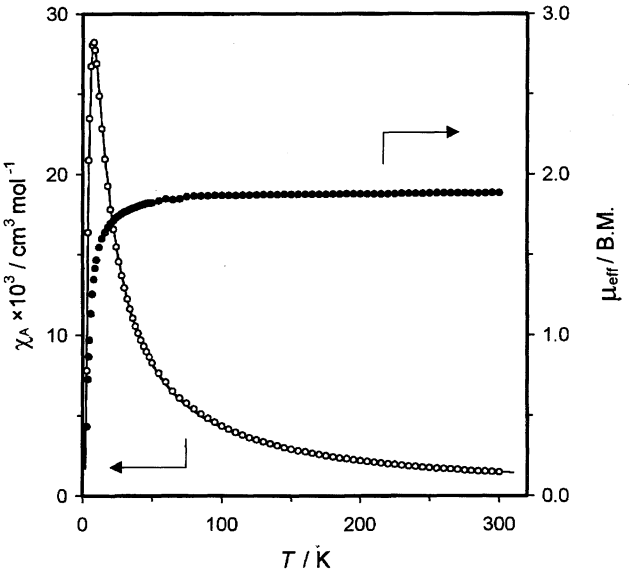

Fig. 5. Temperature dependence of magnetic susceptibilities (○) and magnetic moments (●) for **2**. The solid curve was obtained as described in the text.

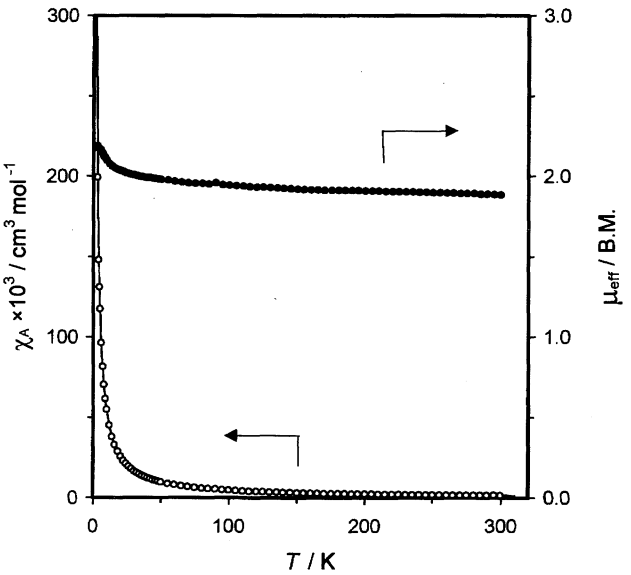

Fig. 6. Temperature dependence of magnetic susceptibilities (○) and magnetic moments (●) for **3**.

Hamiltonian, $\mathcal{H} = -2JS_1 \cdot S_2$, for $S_1 = S_2 = 1/2$, and the other symbols have their usual meanings. The best-fit parameters of $2J$ and g were obtained by a nonlinear least-squares procedure, in which $N\alpha$ is fixed at 60×10^{-6} $cm^3\,mol^{-1}$. The quality of the fit was estimated by means of a discrepancy index (σ_{dis}),

$$\sigma_{dis} = \sqrt{\frac{\sum(\chi_{obsd}-\chi_{calcd})^2}{\sum\chi_{obsd}^2}}. \qquad (2)$$

The values of $2J$, g, μ_{eff} (at room temperature), and σ_{dis} are summarized in Table 6. These magnetic data suggest that a weak antiferromagnetic interaction ($2J = -5$——-13 cm^{-1}) is operative in **1**, **2**, **4**, **5**, and **6**, whereas a weak ferromagnetic interaction ($2J = 9$ cm^{-1}) is operative in **3**. Furthermore, for **3**, the field dependence of the molar magnetization (M) was

Table 6. Magnetic Data for **1**—**6**

Complex	g	$2J/cm^{-1}$	μ_{eff}/B.M. (T/K)	$\sigma_{dis} \times 10^2$
1	2.23	−13	1.91 (294.8)	0.48
2	2.16	−9	1.88 (299.9)	1.42
3	2.19	9	1.88 (299.9)	0.37
4	2.21	−8	1.89 (295.0)	0.65
5	2.19	−7	1.88 (299.5)	0.57
6	2.15	−5	1.85 (299.5)	0.71

measured to confirm the ferromagnetically coupled triplet ground state. The M vs. H plots are shown in Fig. 7. The molar magnetization plots are in approximately agreement with the equation $M = g\beta SNBs(x)$ with $S = 1$ and $g = 2.19$, where $Bs(x)$ is the Brillouin function[35] defined by

$$Bs(x) = \frac{(2S+1)}{2S}\coth\left[\left(\frac{2S+1}{2S}\right)x\right] - \frac{1}{2S}\coth\left(\frac{x}{2S}\right)$$
$$\text{with } x = \frac{g\beta SH}{kT}, \quad (3)$$

indicating that the magnetic interaction in **3** yields a triplet ground state and a singlet excited state.

The magnitude of antiferromagnetic interaction in triply carboxylato-bridged complexes **1**, **2**, **4**, **5**, and **6** are much less than those found for quadruply carboxylate-bridged complexes, $[\{Cu(RCOO)_2L\}_2]$,[2—4] and are still less than those found for doubly carboxylato-bridged complexes, $[\{Cu(RCOO)(phen \text{ or } bpy)(L)\}_2]X_2$.[10,28] However, it is remarkable that the ferromagnetic coupling in **3** is almost equivalent compared to that for $[Cu_2(CH_3COO)_3(bpy)_2]ClO_4$ ($2J = 7.2$ cm^{-1}) with the type-B structure.[11]

It is worth investigating the correlation of the structure (especially the coordination geometry around copper(II) ion and the bridging mode) with the magnetism in triply carboxylato-bridged complexes. In the type-A complexes, in which two copper(II) ions are linked by two *monatomic* bridging

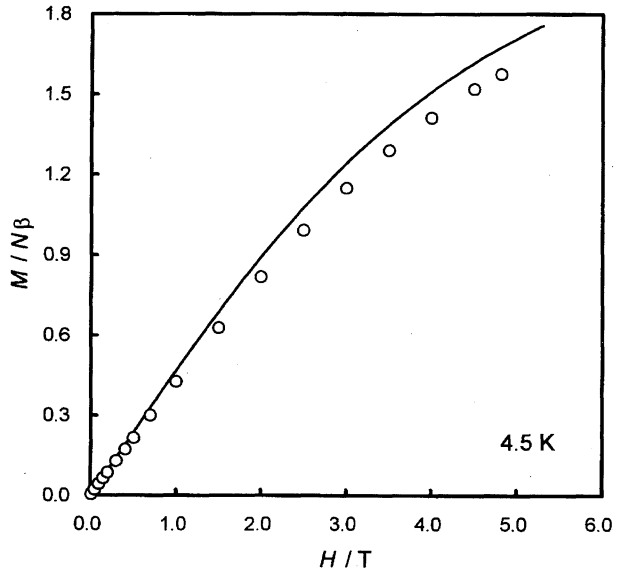

Fig. 7. Field dependence of the magnetization for **3** at 4.5 K. The solid curve ($S = 1$, $g = 2.19$) was obtained as described in the text.

carboxylates and one bidentate *syn–syn* carboxylate, three pathways are provided for the superexchange interaction between copper(II) ions. The geometry of these copper(II) ions are SP and the *syn–syn* carboxylato ligand connects each basal coordination site of copper(II) ions. Thus, the *syn–syn* carboxylate ion, oriented to the dx^2–y^2 magnetic orbital containing the unpaired spin density, can be considered as a primary pathway of spin-exchange interaction. In addition, a weak exchange interaction may also operate in the out-of-plane type of a framework (Cu_2O_2 moiety) consisting of two *monatomic* carboxylato-bridging, because of the very small unpaired spin density on the apical site of copper(II) ion. Chiari and co-workers[23,24] reported on the magnetic and structural properties of a series of dinuclear copper(II) complexes, in which copper(II) ions are doubly bridged by two *monatomic* bridging carboxylates in an out-of-plane fashion. Although most of those complexes exhibit a weak antiferromagnetic interaction ($2J$ = ca.-3 cm^{-1}), a weak ferromagnetic coupling ($2J = 1.3$ cm^{-1}) was found in $[\{CuX(CH_3COO)\}_2]\cdot H_2O\cdot C_2H_5OH$ {X = anion of *N*-(1,1-dimethyl-2-hydroxyethyl)salicylaldimine}.[36] Regarding the magnetic behavior of this complex, Chiari et al.[24] have pointed out that the low planarity of the Cu_2O_2 bridging unit diminishes antiferromagnetic interactions, and that net ferromagnetic coupling was observed; because the complex $[\{CuX(CH_3COO)\}_2]\cdot H_2O\cdot C_2H_5OH$ did not have any inversion centers, the Cu_2O_2 bridging unit was not strictly planar and the basal planes were not parallel each other. In the type-A complexes, the Cu_2O_2 bridging unit is also not strictly planar (dihedral angles between the Cu1–O3···O5 and the Cu2–O5···O3 planes are 148.5° and 147.4° for **1** and **2**, respectively), hence a weak ferromagnetic interaction is predicted. Consequently, the observed antiferromagnetic coupling ($2J = -13$——-9 cm^{-1}) for **1** and **2** are dominantly mediated by the *syn–syn* bridging carboxylate.

On the other hand, it is more difficult to give a reasonable explanation for the magnetism of the type-B complexes with complicated bridging systems. The weak antiferromagnetic or ferromagnetic interactions ($2J = -8$——9 cm^{-1}) was evaluated for these complexes. Type-B complexes **3**—**6** with one *monatomic* bridging carboxylate and two bidentate *syn–syn* carboxylates have different geometries around two copper(II) ions in each dinuclear complex; one copper(II) ion has a pseudo SP geometry ($\tau = 0.06$—0.17) and the other has a fairly distorted SP geometry ($\tau = 0.28$—0.39). The oxygen atom (O1) of the *monatomic* bridging carboxylate simultaneously occupies an edge of the basal coordination plane of the Cu1 site and the apex of the Cu2 site. Similarly, oxygen atoms O5 and O6 of one *syn–syn* bridging carboxylate coordinate to the apical site of Cu1 and a basal site of Cu2, respectively. Hence, the spin-exchange interaction is mainly propagated through the other *syn–syn* carboxylate group (O3–C3–O4) connected between the robes of the dx^2–y^2 magnetic orbital. (Even if the coordination geometry of the Cu2 site is assigned to a strongly distorted TBP, the robe of the dz^2 magnetic orbital along the trigonal axis is directed to O4.) This situation is very similar to that in

$\{[Cu_2(PhCOO)_3(bppz)]ClO_4 \cdot (H_2O)_2\}_n$.[27]

It is of particular interest that a net ferromagnetic interaction was observed in only **3**. Recently, several structural-parameters, e.g. the bending angle between the least-squared Cu–O···O–Cu plane and the O–C–O plane,[7] the Cu–O–C angle,[37] and the Cu–O–C–O torsion angle,[27] which influence the strength of antiferromagnetic interaction in carboxylato-bridged dicopper complexes, have been proposed. The relationship between the structural parameters and the $2J$ values for the present complexes were carefully inspected. Unfortunately, an apparent correlation could not be found between the specific structural-parameter and the $2J$ values in each series. However, the bending angle (12.6°), the average Cu–O–C angle (133.3°), and the Cu–O–C–O torsion angles (19(1)°, −13(1)°) in **3** are all larger than those of the other complexes. Since the torsion of the carboxylato-bridge participated in the exchange interaction is large in **3**, the antiferromagnetic coupling has probably diminished most.

According to Hoffmann's theory,[38] the singlet-triplet energy separation ($2J$) for the copper(II) dimer can be represented as the sum of a ferromagnetic term ($2J_F$) and an antiferromagnetic term ($2J_{AF}$):

$$2J = 2J_F + 2J_{AF}. \quad (4)$$

In comparison within a series of structurally related complexes, the $2J_F$ term is considered to be virtually invariant.[5,38,39] On the other hand, the $2J_{AF}$ term is considered to be proportional to the square of the energy gap between the two singly occupied molecular orbitals (SOMO's), and especially depends on the molecular structure.[5,38,39] The singlet–triplet energy separation results from a competition between two terms. Although magnetic data for the present complexes suggest that the ferromagnetic contribution and the antiferromagnetic contribution are almost comparable, slight changes in various structural-parameters of the present complexes cause a very small variation in the singlet–triplet energy separation. Consequently, the net ferromagnetic interaction was observed for **3** owing to a weaker antiferromagnetic contribution derived from a large distortion of the Cu–O–C–O–Cu super-exchange pathway.

This work was supported by a Grant-in-Aid for Scientific Research (B) No.10440196 and a Grant-in-Aid for Scientific Research on Priority Areas No.10149240 "Metal-assembled Complexes" from the Ministry of Education, Science, Sports and Culture.

References

1) D. J. Hodgson, *Prog. Inorg. Chem.*, **19**, 173 (1975); V. H. Crawford, H. W. Richardson, J. R. Wasson, D. J. Hodgson, and W. E. Hatfield, *Inorg. Chem.*, **15**, 2107 (1976).

2) R. J. Doedens, *Prog. Inorg. Chem.*, **21**, 209 (1976).

3) M. Melník, *Coord. Chem. Rev.*, **42**, 259 (1982).

4) M. Kato and Y. Muto, *Coord. Chem. Rev.*, **92**, 45 (1988).

5) O. Kahn, *Angew. Chem., Int. Ed. Engl.*, **24**, 834 (1985).

6) L. K. Thompson, F. L. Lee, and E. J. Gabe, *Inorg. Chem.*, **27**, 39 (1988).

7) M. Yamanaka, H. Uekusa, S. Ohba, Y. Saito, S. Iwata, M. Kato, T. Tokii, Y. Muto, and O. W. Steward, *Acta Crystallogr., Sect. B*, **47B**, 344 (1991); T. Kawata, H. Uekusa, S. Ohba, T. Furukawa, T. Tokii, Y. Muto, and M. Kato, *Acta Crystallogr., Sect. B*, **48B**, 253 (1992).

8) S. Meenakumari, S. K. Tiwari, and A. R. Chakravarty, *J. Chem. Soc., Dalton Trans.*, **1993**, 2175; K.-S. Bürger, P. Chaudhuri, and K. Wieghardt, *J. Chem. Soc., Dalton Trans.*, **1996**, 247.

9) T. Tokii, S. Nakahara, N. Hashimoto, M. Koikawa, M. Nakashima, and H. Matsushima, *Bull. Chem. Soc. Jpn.*, **68**, 2533 (1995).

10) T. Tokii, N. Watanabe, M. Nakashima, Y. Muto, M. Morooka, S. Ohba, and Y. Saito, *Chem. Lett.*, **1989**, 1671; *Bull. Chem. Soc. Jpn.*, **63**, 364 (1990).

11) G. Christou, S. P. Perlepes, E. Libby, K. Folting, J. C. Huffman, R. J. Webb, and D. N. Hendrickson, *J. Chem. Soc., Chem. Commun.*, **1990**, 746; *Inorg. Chem.*, **29**, 3657 (1990).

12) R. L. Rardin, W. B. Tolman, and S. J. Lippard, *New J. Chem.*, **15**, 417 (1991), and references therein.

13) H. Matsushima, M. Koikawa, M. Nakashima, and T. Tokii, *Chem. Lett.*, **1995**, 869.

14) P. W. Selwood, "Magnetochemistry," Interscience Publishers, New York (1956), pp. 78 and 91.

15) C. J. Gilmore, "MITHRIL," *J. Appl. Crystallogr.*, **17**, 42 (1984); M. C. Burla, M. Camalli, G. Cascarano, C. Giacovazzo, G. Polidori, R. Spagna, and D. Viterbo, "SIR," *J. Appl. Crystallogr.*, **22**, 389 (1989); P. T. Beurskens, "DIRDIF," Tech. Rep. 1984/1, Crystallography Laboratory, Toernooiveld, 6525 ed, Nijmegen, Netherlands.

16) Function minimized: $\Sigma w(|F_o| - |F_c|)^2$, where $w = 4F_o^2/\sigma^2(F_o^2)$. Standard deviation of an observation of unit weight: $[\Sigma w(|F_o| - |F_c|)^2/(N_o - N_v)]^{1/2}$, where N_o = number of observations, N_v = number of variables.

17) D. T. Cromer and J. T. Waber, "International Tables for X-Ray Crystallography," Kynoch Press, Birmingham (1974), Vol. 4, Table 2.2A.

18) J. A. Ibers and W. C. Hamilton, *Acta Crystallogr.*, **17**, 781 (1964).

19) D. T. Cromer, "International Tables for X-Ray Crystallography," Kynoch Press, Birmingham (1974), Vol. 4, Table 2.3.1.

20) "TEXSAN- TEXRAY Structure Analysis Package," Molecular Structure Corporation, Houston, TX (1985).

21) A. W. Addison, T. N. Rao, J. Reedijk, J. van Rijn, and G. C. Verschoor, *J. Chem. Soc., Dalton Trans.*, **1984**, 1349.

22) Rardin et al. have reported only the crystal structure of the complex with this bridging linkages as unpublished results in Ref. 12.

23) B. Chiari, J. H. Helms, O. Piovesana, T. Tarantelli, and P. F. Zanazzi, *Inorg. Chem.*, **25**, 870 (1986).

24) B. Chiari, J. H. Helms, O. Piovesana, T. Tarantelli, and P. F. Zanazzi, *Inorg. Chem.*, **25**, 2408 (1986), and references therein.

25) R. Hämäläinen, M. Ahlgren, and U. Trupeinen, *Acta Crystallogr., Sect. B*, **38B**, 1577 (1982).

26) W. B. Tolman, S. Liu, J. G. Bentsen, and S. J. Lippard, *J. Am. Chem. Soc.*, **113**, 152 (1991); M. Osawa, U. P. Singh, M. Tanaka, Y. Moro-oka, and M. Kitajima, *J. Chem. Soc., Chem. Commun.*, **1993**, 310; H. E. Wages, K. L. Taft, and S. J. Lippard, *Inorg. Chem.*, **23**, 4985 (1993); X.-M. Chen, Y.-X. Tong, and T. C. W. Mak, *Inorg. Chem.*, **33**, 4586 (1994); H. Matsushima, E. Ishiwa, M. Koikawa, M. Nakashima, and T. Tokii, *Chem. Lett.*, **1995**, 129.

27) A. Neels, H. Stoeckli-Evans, A. Escuer, and R. Vicente, *Inorg. Chim. Acta*, **260**, 189 (1997).

28) E. Duber, U. K. Häring, K. H. Scheller, P. Baltzer, and H. Sigel, *Inorg. Chem.*, **23**, 3785 (1984); S. P. Perlepes, J. C. Huffman, and G. Christou, *Polyhedron*, **11**, 1471 (1992); S. Meenakumari and A. R. Chakravarty, *Polyhedron*, **12**, 347 (1993); R. Costa, C. López, E. Molins, and E. Espinosa, *Inorg. Chem.*, **37**, 5686 (1998).

29) M. S. Haddad, S. R. Wilson, D. J. Hodgson, and D. N. Hendrickson, *J. Am. Chem. Soc.*, **103**, 384 (1981); J. E. Plowman, T. M. Loehr, C. K. Schauer, and O. P. Anderson, *Inorg. Chem.*, **23**, 3553 (1984); T. Tokii, K. Ide, M. Nakashima, and M. Koikawa, *Chem. Lett.*, **1994**, 441.

30) T. Tokii, M. Nagamatsu, H. Hamada, and M. Nakashima, *Chem. Lett.*, **1992**, 1091.

31) G. B. Deacon and R. J. Phillips, *Coord. Chem. Rev.*, **33**, 227 (1980); K. Nakamoto, "Infrared and Raman Spectra of Inorganic and Coordination Compounds," 4th ed, Wiley-Interscience, New York (1986), pp. 231—233.

32) A. A. G. Tomlinson, B. J. Hathaway, D. E. Billing, and P. Nicholls, *J. Chem. Soc. A*, **1969**, 65; W. D. Harrison, D. M. Kennedy, M. Power, R. Sheahan, and B. J. Hathaway, *J. Chem. Soc., Dalton Trans.*, **1981**, 1556; S. Tyagi and B. J. Hathaway, *J. Chem. Soc., Dalton Trans.*, **1983**, 199.

33) S. P. Perlepes, J. C. Huffman, G. Christou, and S. Paschalidou, *Polyhedron*, **14**, 1073 (1995).

34) B. Bleaney and K. D. Bowers, *Proc. R. Soc. London, Ser. A*, **214**, 451 (1952).

35) R. L. Carlin, "Magnetochemistry," Springer-Verlag, Berlin (1986).

36) A. M. Greenaway, C. J. O'Connor, J. W. Overman, and E. Sinn, *Inorg. Chem.*, **20**, 1508 (1981).

37) K.-S. Bürger, P. Chaudhuri, and K. Wieghardt, *Inorg. Chem.*, **35**, 2704 (1996).

38) P. J. Hay, J. C. Thibeault, and R. Hoffmann, *J. Am. Chem. Soc.*, **97**, 4884 (1975).

39) O. Kahn, "Molecular Magnetism," VCH Publishers, New York (1993).